Project Report
NASA/L-4

Turbulence Climatology at Dallas/Ft. Worth (DFW) Airport—Implications for a Departure Wake Vortex Spacing System

G. H. Perras
T. J. Dasey

30 November 2000

Lincoln Laboratory
MASSACHUSETTS INSTITUTE OF TECHNOLOGY
LEXINGTON, MASSACHUSETTS

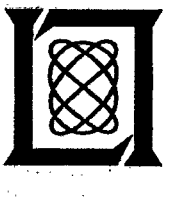

Prepared for the National Aeronautics and Space Administration
Langley Research Center, Hampton, Virginia 23681-2199.

This document is available to the public through
the National Technical Information Service,
Springfield, Virginia 22161.

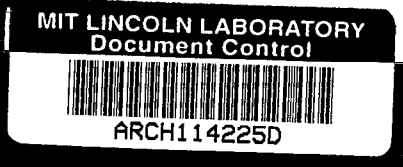

TECHNICAL REPORT STANDARD TITLE PAGE

1. Report No.	2. Government Accession No.	3. Recipient's Catalog No.
NASA/L-4		

4. Title and Subtitle	5. Report Date
Turbulence Climatology at Dallas/Ft. Worth (DFW) Airport—Implications for a Departure Wake Vortex Spacing System	30 November 2000
	6. Performing Organization Code

7. Author(s)	8. Performing Organization Report No.
G.H. Perras and T.J. Dasey	NASA/L-4

9. Performing Organization Name and Address	10. Work Unit No. (TRAIS)
MIT Lincoln Laboratory 244 Wood Street Lexington, MA 02420-9108	11. Contract or Grant No. NASA Langley

12. Sponsoring Agency Name and Address	13. Type of Report and Period Covered
National Aeronautics and Space Administration Langley Research Center Hampton, VA 23681-2199	Project Report
	14. Sponsoring Agency Code

15. Supplementary Notes

This report is based on studies performed at Lincoln Laboratory, a center for research operated by Massachusetts Institute of Technology, under Air Force Contract F19628-00-C-0002 to NASA Langley Research Center.

16. Abstract

Potential adaptive wake vortex spacing systems may need to rely on wake vortex decay rather than wake vortex transport in reducing wake separations. A wake vortex takeoff-spacing system in particular will need to rely on wake decay. Ambient turbulence is the primary influence on wake decay away from the ground. This study evaluated 18 months of ambient turbulence measurements at Dallas/Ft. Worth (DFW) Airport. The measurements show minor variation in the turbulence levels at various times of the year or times of the day for time periods when a departure system could be used. Arrival system operation was also examined, and a slightly lower overall turbulence level was found as compared to departure system benefit periods. The Sarpkaya model, a validated model of wake vortex behavior, was applied to various turbulence levels and compared to the DFW turbulence statistics. The results show that wake vortices from Heavy aircraft on takeoff should dissipate within one minute for the majority of the time and will rarely last two minutes. These results will need to be verified by wake vortex measurements on departure.

17. Key Words	18. Distribution Statement
turbulence, vortex, eddy, decay, dissipation, DFW, wake	This document is available to the public through the National Technical Information Service, Springfield, VA 22161.

19. Security Classif. (of this report)	20. Security Classif. (of this page)	21. No. of Pages	22. Price
Unclassified	Unclassified	34	

FORM DOT F 1700.7 (8-72) Reproduction of completed page authorized

ABSTRACT

Potential adaptive wake vortex spacing systems may need to rely on wake vortex decay rather than wake vortex transport in reducing wake separations. A wake vortex takeoff-spacing system in particular will need to rely on wake decay. Ambient turbulence is the primary influence on wake decay away from the ground. This study evaluated 18 months of ambient turbulence measurements at Dallas/Ft. Worth (DFW) Airport. The measurements show minor variation in the turbulence levels at various times of the year or times of the day for time periods when a departure system could be used. Arrival system operation was also examined, and a slightly lower overall turbulence level was found as compared to departure system benefit periods. The Sarpkaya model, a validated model of wake vortex behavior, was applied to various turbulence levels and compared to the DFW turbulence statistics. The results show that wake vortices from Heavy aircraft on takeoff should dissipate within one minute for the majority of the time and will rarely last two minutes. These results will need to be verified by wake vortex measurements on departure.

TABLE OF CONTENTS

LIST OF ILLUSTRATIONS

LIST OF ILLUSTRATIONS (CONTINUED)

1. INTRODUCTION

Aircraft wake vortices are strongly counter-rotating tubes of air that are generated from aircraft as a consequence of the lift on the aircraft. The safety concern of wake vortices, particularly when lighter aircraft are following heavy planes, has caused the Federal Aviation Administration (FAA) to enact minimum separation requirements during the landing and takeoff phases of flight. Decades of past wake vortex measurements clearly show that current wake vortex separations are over-conservative in many weather conditions, and that adapting the separations to the current weather could safely reduce these separations (Hallock, et al., 1998).

The Aircraft Vortex Spacing System (AVOSS) is a NASA Langley Research Center effort aimed at developing the technology for an automated system for adaptively reducing aircraft wake separations (Hinton, et al., 2000 and Perry, et al., 1997). The technology being developed for AVOSS, in the form of improved physical models of vortex behavior, wake vortex sensor technology, and efficient measurement of relevant meteorological variables, is applicable to both the departure and arrival problems. The focus of the application of the AVOSS technology has thus far been toward reducing arrival separations. As part of the AVOSS effort, MIT Lincoln Laboratory has installed meteorological data collection and processing systems at Memphis International Airport (MEM) from 1994-1997 (Dasey, et al., 1997) and more recently at Dallas/Ft. Worth International Airport (DFW) from 1997-2000 (Dasey, et al., 1998).

The ambient wind, along with the wind from the other wing's counter-rotating wake, transport wake vortices after they are generated. Each wake also decays from its initial circulation strength. For some applications, accounting for wake motion and ignoring whether the wake has decayed sufficiently can realize the majority of the benefit of a wake vortex advisory system. An example of this would be a parallel runway arrival application. In this case the main concern is whether the wake moves from one flight path to the flight path of the parallel runway. For most parallel runway separation distances, the crosswind is sufficiently low so that wakes blowing over to the adjacent runway are unusual.

The applications that will need to rely on understanding and measuring wake vortex decay are the in-trail separations on arrival and departure (Dasey, 1998). Particularly on departure, where the exact flight path of the next aircraft is not as well known ahead of time, relying solely on vortex transport in the system implementation is likely to strongly reduce the

amount of time that such a system could be used. In this case understanding the wake vortex decay would give only a marginally-increased benefit. In the single-runway arrival application, wake decay can be the primary consideration when the runway crosswind is light; however, considerable benefit can be realized by detecting wake transport only.

Wake vortices decay faster when interacting with the ground or when exposed to high levels of atmospheric turbulence. One limitation in analyzing the benefits of wake vortex spacing systems and in simulating revised air traffic procedures is the lack of a climatologically representative data set of ambient turbulence measurements.

This report presents a statistical analysis of DFW turbulence estimates during periods of time when reduced arrival and departure wake spacings would likely be possible. A description of the estimation of the eddy dissipation rate (ε), the turbulence parameter used in this study, is given in section 2. Section 3 presents the results of the turbulence analysis for a fourteen-month data set from DFW. Section 4 applies the eddy dissipation rate statistics in section 3 to an out-of-ground-effect model of wake vortex decay. Using departure aircraft weights and airspeeds, an estimate is made of the fraction of time that the models predict that the wakes should decay prior to the next aircraft passage. The departure application is emphasized here because of the simpler implementation path when compared to arrival applications.[1]

---

1 This is largely due to the difficult weather forecasting problem that must be solved for an arrival application. The departure application also has the advantage that it could be applied in Visual Meteorological Conditions (VMC) as well as Instrument Meteorological Conditions (IMC).

2. TURBULENCE ESTIMATION

In support of the development and testing of the AVOSS, an extensive meteorological sensor suite was constructed at the DFW airport (Dasey, et al., 1998). A 150-foot instrumented tower on the airport grounds holds two sonic anemometers. One is located 5 meters above ground level (AGL) and the other at 40 meters. These instruments are used to collect three-dimensional winds at a 10Hz rate. From these data, the eddy dissipation rates (ε) for this study were calculated.

Applied Technologies, Inc. of Boulder, CO, manufactured the sonic anemometers. These sensors transmit and receive a sonic signal along a fixed orthogonal direction. From this, the components of the wind are determined. The measurement range of these sonic anemometers is +/- 15 m/s for the three-axis winds with an accuracy of +/- 0.05 m/s.

Data from the sonic anemometers began being saved in August 1997 and continued until August 2000. The data discussed in this report were based on measurements from August 1997 through December 1998. There was a time period that was void of data that lasted from August 7, 1998 through September 13, 1998. As a result, both August and September have less available data than the other months of the year.

Calculations of eddy dissipation rates were generated by a spectral analysis of the wind data from the sonic anemometers. The wind vector is first rotated so that the U-component is aligned in the direction of the mean wind over the averaging period. In this report the mean wind direction over this period is referred to as the U′ direction, and V′ and W′ are the mostly horizontal and vertical directions orthogonal to U′. Although the V′ and W′ wind components were also analyzed, only the U′ results are discussed in this study.

The power spectrum (S) of the U′ wind component is computed as

$$S = N\tau \left| FFT(U' - \mu_{U'}) \right|^2 / 2\pi$$

where N is the number of samples in the time series, τ is the sampling period (0.1 sec), and $\mu_{U'}$ is the mean of the U′ component over the sampling period. Each spectrum is then smoothed in frequency by a rectangular frequency window whose width varies logarithmically with increasing frequency.

The inertial subrange of each power spectrum is determined automatically by examining a log-log relationship between the power spectrum S and the wavenumber κ defined as

$$\kappa = {2\pi f}/{\mu_{U'}}$$

where f is the spatial frequency. The analysis software looks for a linear portion of the spectrum with a slope near the -5/3 slope predicted by Kolmogorov. Figure 1 shows an example spectrum and the automatically-identified inertial subrange.

The eddy dissipation rate (ε) is then computed by taking all of the points from the power spectrum in the inertial subrange and computing as

$$\varepsilon = \left(\frac{1}{N_I}\right)\sum_{j=1}^{I}\left(\frac{S_j \kappa_j^{5/3}}{C}\right)^{3/2}$$

where N_I is the number of frequency bins in the inertial subrange and C=0.52 for the U′ component (Hogstrom, 1996, Vinnichenko, et al., 1980). The epsilon value calculated is the average dissipation rate over all the spectral points in the inertial subrange. Appendix A presents some sample software that computes eddy dissipation rate.

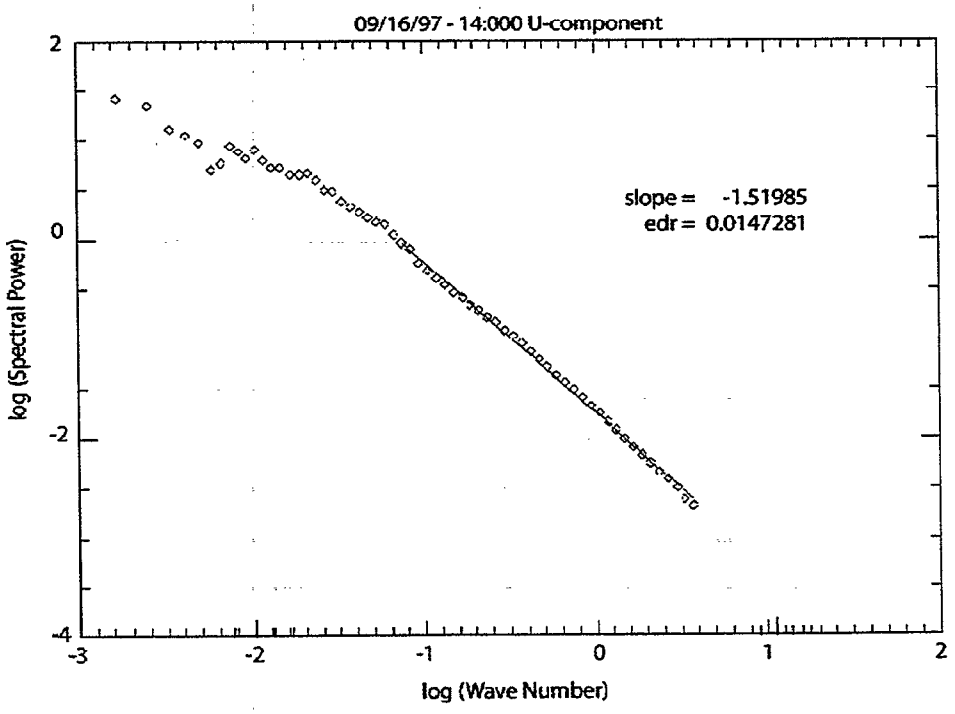

Figure 1. *Example U' power spectrum. The automatically-identified inertial subrange is shown as the solid line overlaying the power spectrum.*

3. DFW TURBULENCE CLIMATOLOGY

Since high turbulence is associated with rapid wake vortex circulation decay, and thus a greater likelihood of being able to reduce separations, the statistical analysis focused on determining when the turbulence was high. Daily and seasonal variation in turbulence was also of interest. The exceedance probability, defined as the probability that the eddy dissipation rate will exceed a given value, was the variable chosen for the majority of the analysis. Specifically, exceedance probabilities were calculated for values in a range from 10^{-7} to 10^{-1}, in increments of $10^{1/2}$.

All of the eddy dissipation rate data presented in this report were calculated using a 30-minute averaging period, as was done in the AVOSS real-time system at DFW. This is because the initial AVOSS software is designed to provide 30-minute predictions of wake vortex behavior. The need for a 30-minute prediction is based on providing ample time for air traffic controllers to be able to safely change the traffic pattern of aircraft arrivals once notified of any changing wake vortex conditions. For a portion of the data set, ε was computed over 5 and 15 minute averages. Unlike using turbulent kinetic energy (TKE) as a measure of turbulence, the eddy dissipation rate value is not biased by the choice of averaging period, as Figure 2 shows.[2]

Although the 5-meter data from the sonic anemometers were analyzed, more attention was given to the 40-meter data. This is because the decay near the ground is not as strongly related to turbulence levels as it is to the destructive influence of ground friction.

---

[2] In some cases, particularly in light wind conditions, a short averaging period may be insufficient to sample a large enough portion of the atmosphere. The result is an inability to compute ε due to a poorly-defined or nonexistent inertial subrange.

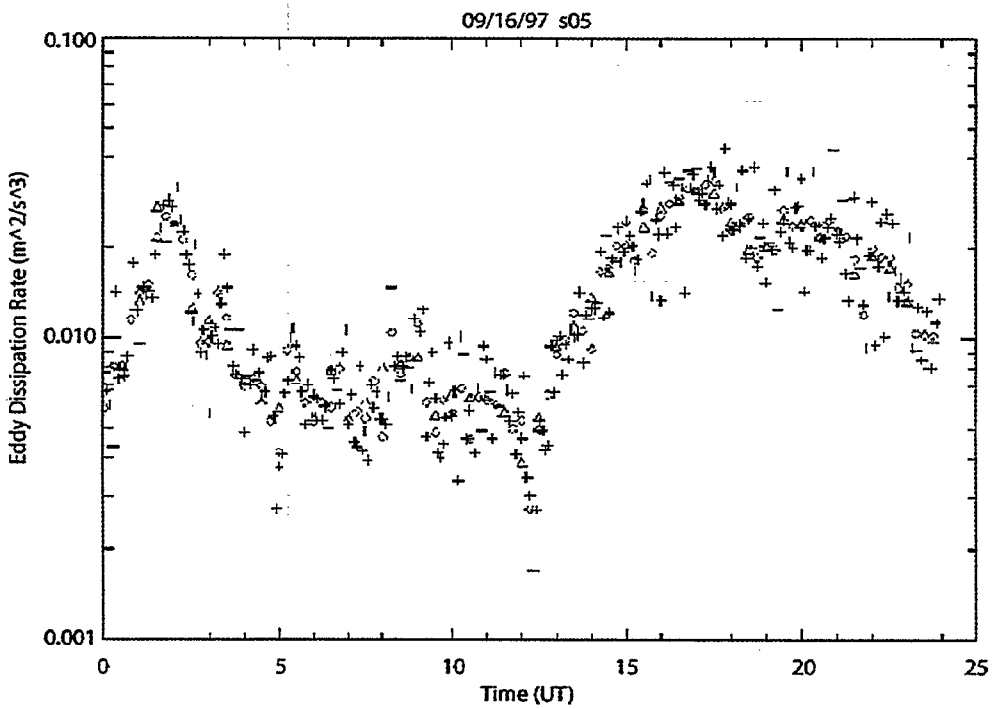

Figure 2. *Example diurnal eddy dissipation rate distribution. The symbols show the calculation of various averaging intervals (triangles = 30 min., diamonds = 15 min., plusses = 5 min.).*

3.1 Statistics for Wake Departure System Operation

A departure wake vortex spacing system could be used during both VMC and IMC conditions. However, during certain types of IMC, notably when thunderstorms or frozen precipitation are present, it is unlikely that wake vortex constraints would have a sizable impact on airport operations. Weather of this type is also likely to be quite variable over short spatial domains, making accurate measurement of the local turbulence values that could affect wake vortices very difficult. The National Weather Service hourly METAR-format observations from the DFW airport were used to exclude all times of thunderstorm activity, moderate or heavy rain, and any type of frozen precipitation.

Along with the restriction of particular weather conditions, the time of day was also considered for defining the times when a departure system would be of benefit. Since passenger traffic is typically very light during the overnight hours, only turbulence data collected between 6AM and 10PM local time were used in generating the results presented in this report, except for those which specifically present the data as a function of hour of day.

Figure 3 compares the exceedance probability curves of eddy dissipation rate for both 5 meters and 40 meters. As one would expect, the values are greater for the 5-meter data than at 40 meters due to increased turbulence near the ground. These curves provide a good indication of typical dissipation rate distributions for DFW.

Figure 4 shows a contour plot for dissipation rate exceedance probabilities for departure system operation by month. This figure shows that there is not a significant amount of variation throughout the year in the range of dissipation rate values. The peak observed values for the year occur in April, but the highest average values for any month occur in June.

Figure 5 is a contour plot similar to Figure 4, but the time scale is by hour of day instead of month. Somewhat surprisingly, the occurrence of the higher dissipation rates remains very steady no matter what the time of day. However, there is a noticeable decrease in the likelihood of smaller values during the afternoon and the range of values decreases. This is expected due to the influence of solar heating.

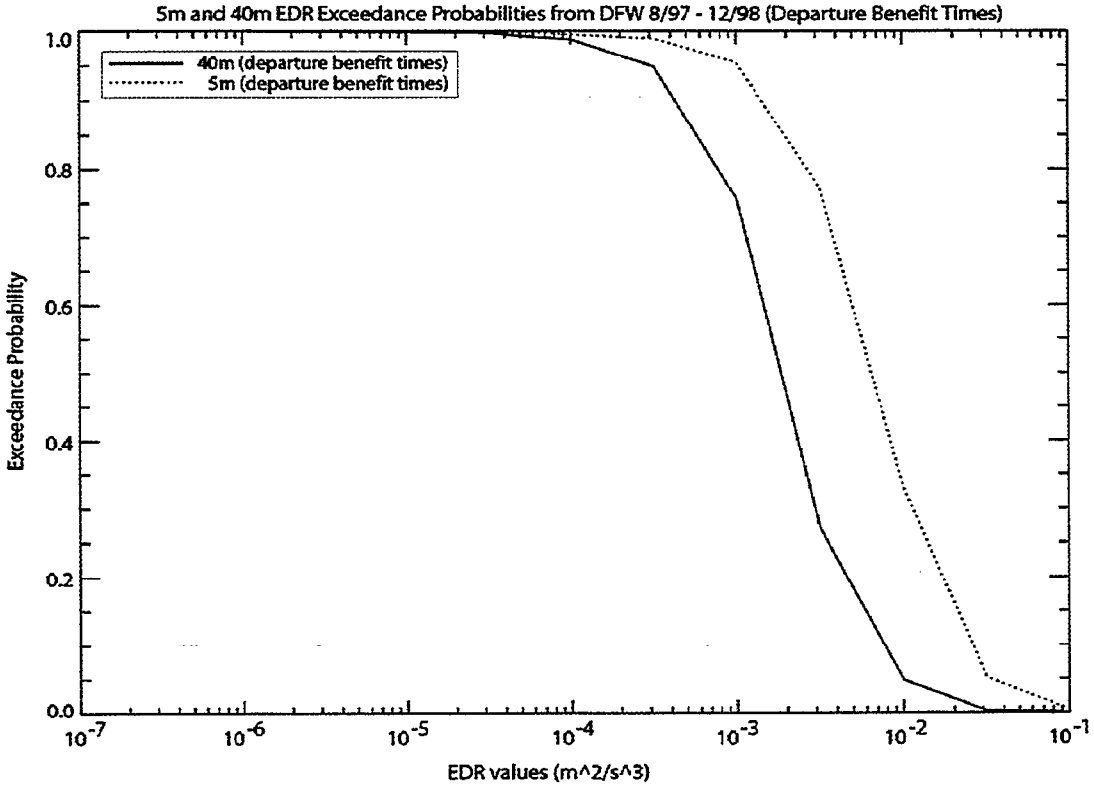

Figure 3. *Distribution of eddy dissipation rate exceedance values at DFW, measured from 40 m and 5 m. The plot shows the statistics from the times that a departure wake spacing system could likely be used.*

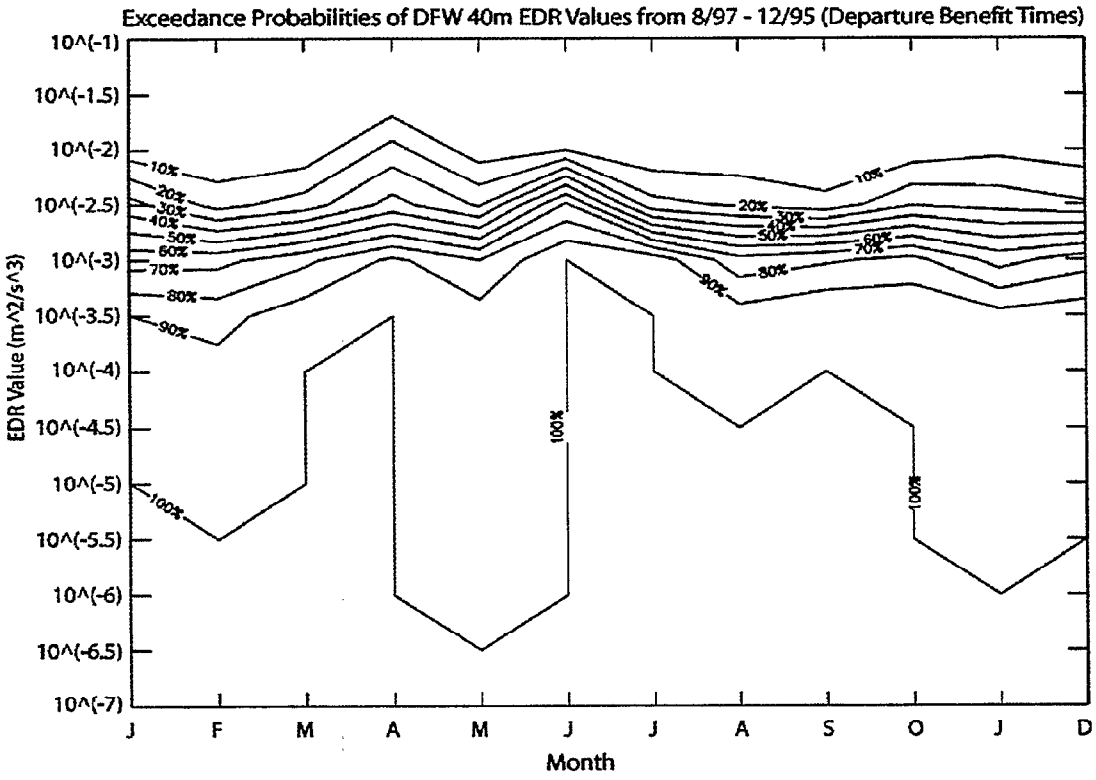

Figure 4. *Contour plot of ε exceedance values as a function of the month of the year. The plot shows the statistics from the times that a departure wake spacing system could likely be used.*

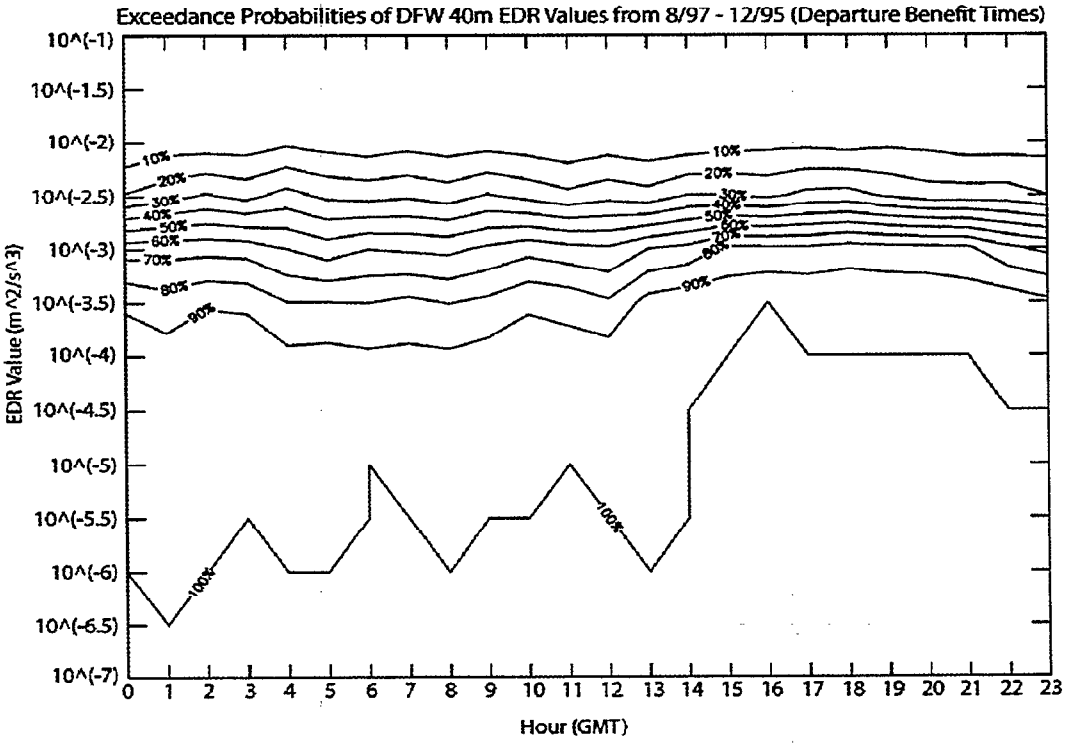

Figure 5. *Contour plot of ε exceedance values as a function of the time of day. The plot shows the statistics from times during which weather conditions would allow the use of a departure wake spacing system.*

3.2 Statistics for Wake Arrival System Operation

An arrival system can only be used when reduced ceiling or visibility conditions prevent visual approaches. During these times, when the pilots are unable to see other nearby aircraft, Air Traffic Control (ATC) assumes sole responsibility for aircraft separation. It is only during these times that arrival wake vortex separations are applied.

The strict definition of Instrument Meteorological Conditions (less than 1000-foot ceiling or 3-mile visibility) is too restrictive. Controllers have expressed that arrival traffic rates begin to be affected at much higher ceilings and visibilities, due to the inability of pilots to navigate visually along at least a portion of the approach. DFW arrival rates begin to be affected by ceilings of 4500 feet or visibilities of about 5 miles. For this turbulence analysis, a modified definition of IMC consisting of a ceiling less than or equal to 2500 feet. or a visibility of less than or equal to 5 miles is used. These modified-IMC times were determined by using the DFW hourly METAR observations. As with the analysis for departure benefits, all periods of thunderstorm activity, moderate or heavy rain, and any frozen precipitation were excluded from consideration. Also, only the hours between 6AM and 10PM were examined, except when data are presented specifically as a function of time of day.

Figure 6 is similar to Figure 1, but with the addition of the probability curves for 5-meter and 40-meter dissipation rates during arrival-system benefit times of modified IMC. The curves very closely match those from the departure data, but the values are somewhat smaller. This is most likely due to less solar radiation to increase turbulence values during the times of modified IMC.

Figure 7 is a contour plot of dissipation rate exceedance probabilities. Just as in Figure 2, which showed probability contours for data during departure-system benefit times, April once again has the peak annual values. However, the increase is much sharper for these modified-IMC times. The contours are very consistent from month to month throughout the rest of the year with the range of values remaining very steady.

Figure 8 shows the data for modified IMC times by hour of day. Notice that the probabilities and range of values are extremely steady throughout the day. This is most likely due to the lack of solar heating during these types of conditions.

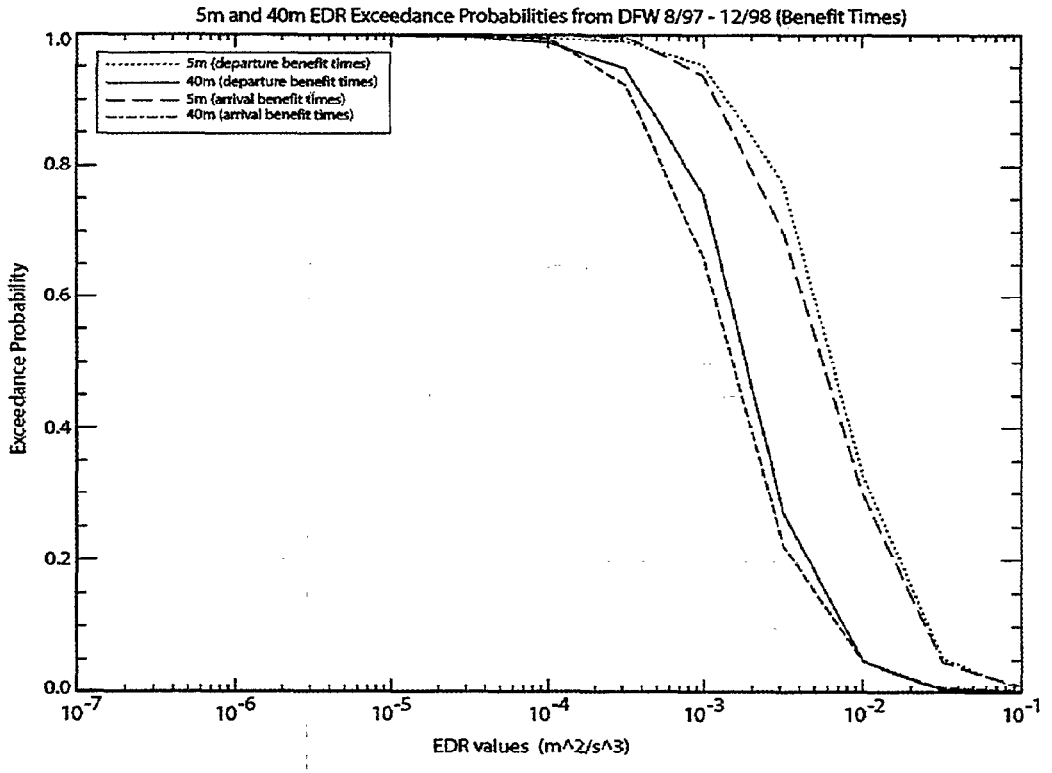

Figure 6. *Distribution of eddy dissipation rate exceedance values at DFW, measured from 40 m and 5 m. . The plot compares the statistics from the times that a departure wake spacing system could likely be used with those times for an arrival system.*

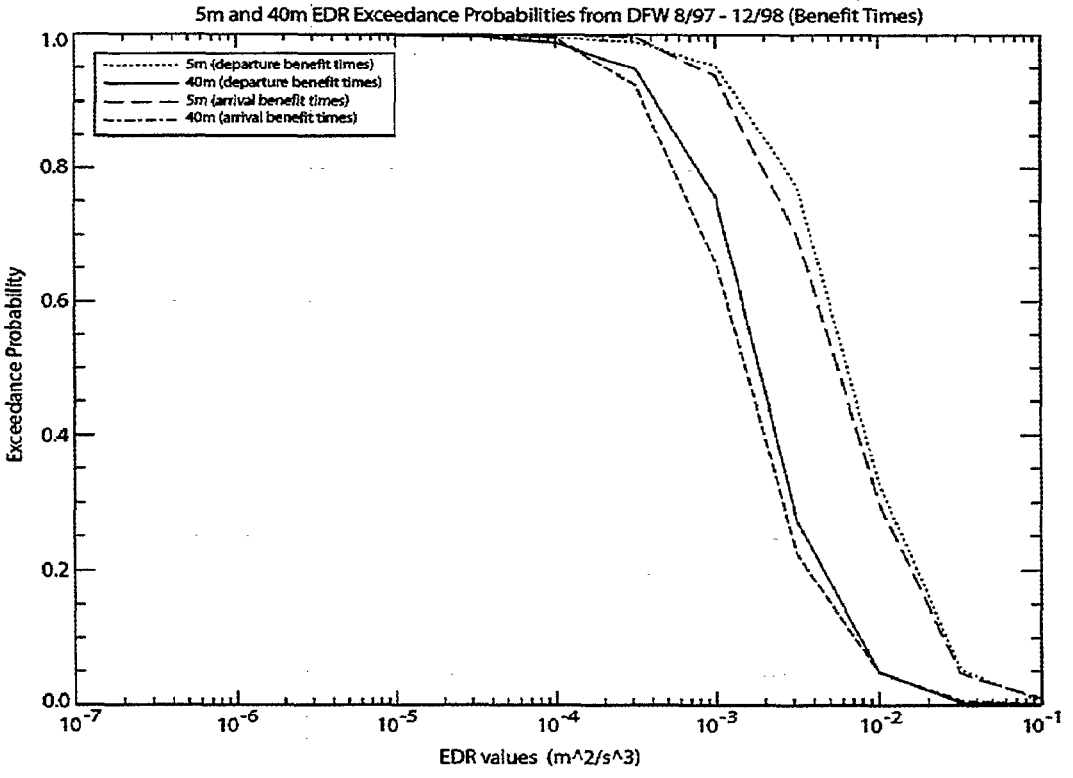

Figure 7. *Contour plot of ε exceedance values as a function of the month of the year. The plot shows the statistics from the times that an arrival wake spacing system could likely be used.*

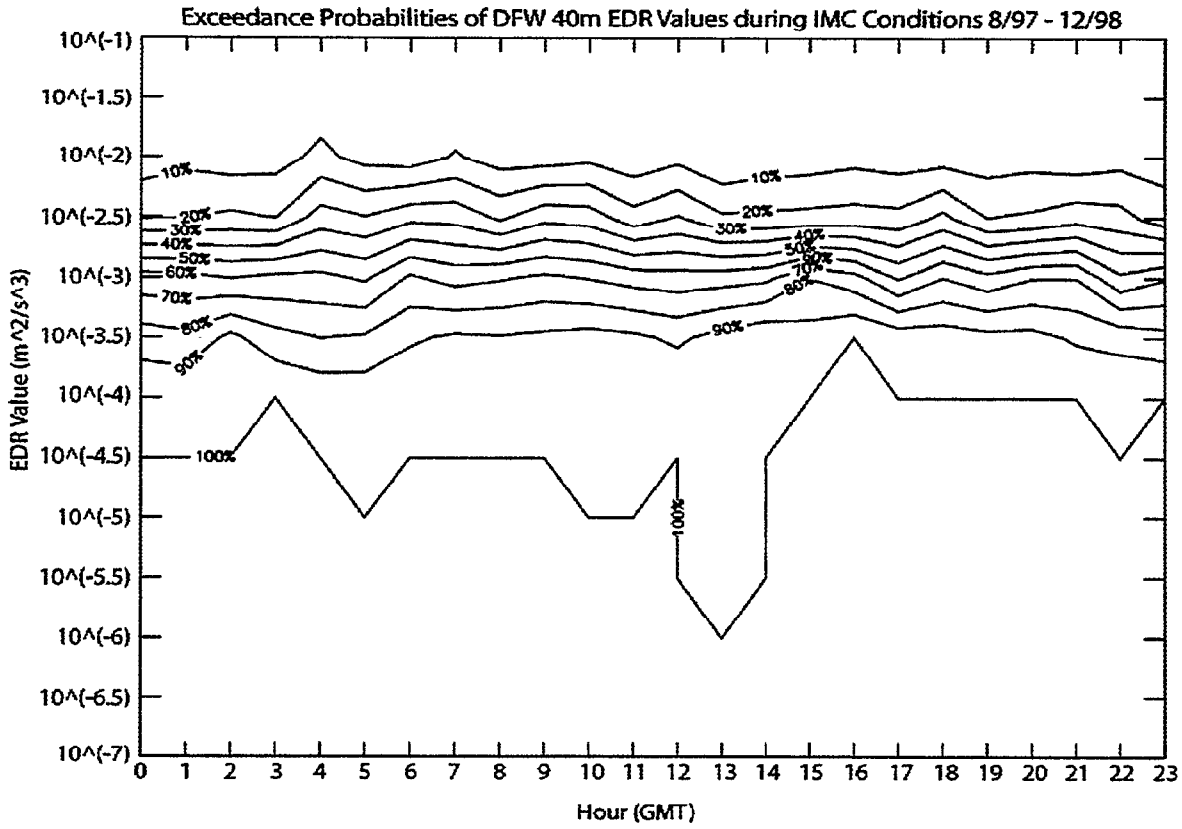

Figure 8. *Contour plot of ε exceedance values as a function of the time of day. The plot shows the statistics from the times during which the weather conditions would allow the use of an arrival wake spacing system.*

4. WAKE VORTEX DEPARTURE MONITOR ASSESSMENT

As mentioned in the Introduction, an in-trail takeoff separation system would need to rely primarily on vortex decay rather than vortex transport for its benefits. This is because the exact flight path of the following aircraft is not known with great certainty. Even if improved navigation and Flight Management Systems (FMS) could reduce this uncertainty, the predicted flight path data would have to be made available from the aircraft to a wake spacing system. Since the primary factor in wake decay away from the ground is atmospheric turbulence, the authors sought to use the results in the previous section to make some preliminary statement about how frequently takeoff separations could be reduced at DFW. This cannot be readily done with measurements since few vortex measurements away from the ground exist for takeoffs.

The eddy dissipation rate climatology presented in the previous section was used to estimate vortex demise probabilities by applying the ε statistics to the Sarpkaya model of vortex decay in the atmosphere (Sarpkaya, 1999). The Sarpkaya model was the wake vortex model chosen for the July 2000 real-time AVOSS experiment at DFW. As with most analytic vortex models, the Sarpkaya model uses nondimensional forms of the weather and vortex variables and also of time. In these representations, the effects of aircraft differences have been removed by normalizing the data by aircraft airspeed, weight, and wingspan. The model then expresses the decay of a generic vortex after these normalizations are applied. The nondimensional form of a variable is indicated in this paper with a * superscript.

Sarpkaya expresses normalized vortex circulation (Γ) as an exponential function of nondimensional time (T), expressed as

$$\Gamma^* = \exp(-\frac{C}{T^*}T).$$

The parameter T* represents the time at which a catastrophic vortex demise event, such as vortex bursting (Lambourne, et al., 1961) or Crow instability (Crow, 1970), takes place. The value of C used in this study is C=0.45. The relationship between vortex demise time and the level of atmospheric turbulence is determined empirically by laboratory and atmospheric measurements. The Sarpkaya model relationship is shown in Figure 9.

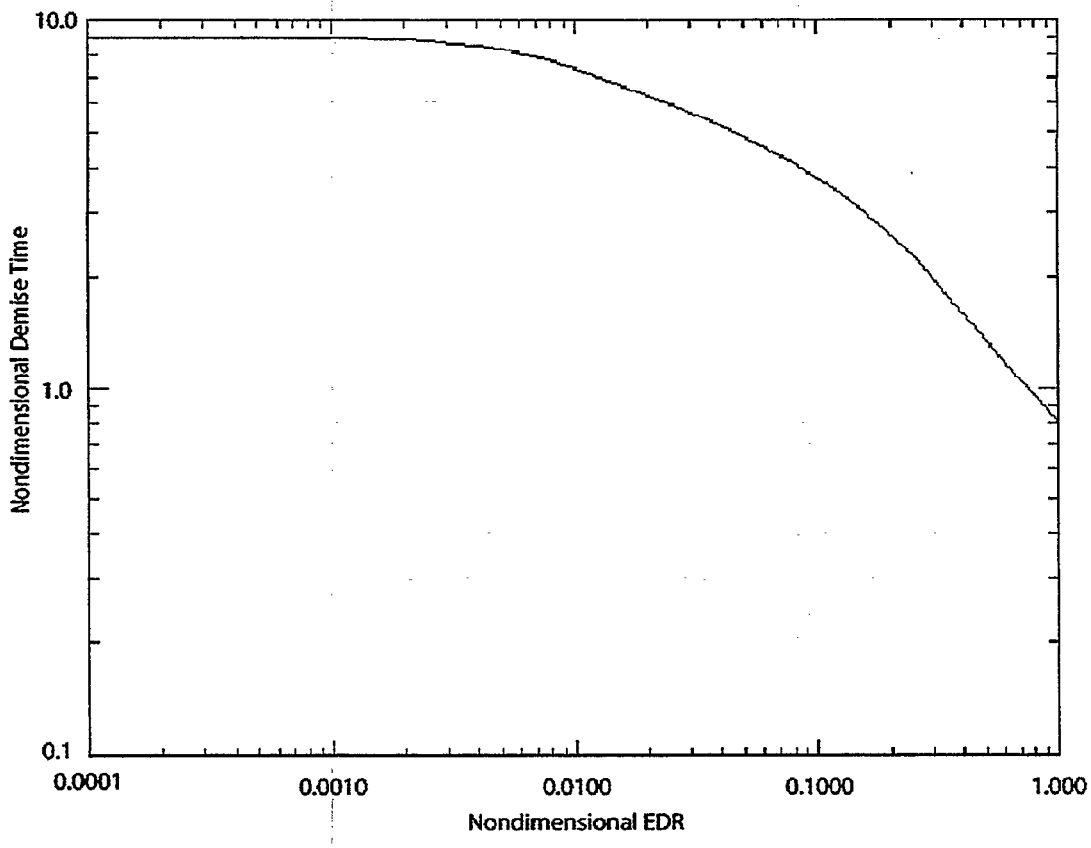

Figure 9. *Plot of the Sarpkaya model relationship between ε^* and T^*.*

To estimate the demise times for particular values of ε, the nondimensionalizations $\varepsilon^* = (\varepsilon b)^{1/3} / V_0$ and $T^* = TV_0 / b$ were applied for most of the commercial aircraft in the Heavy weight category. The symbol b refers to the initial vortex separation (theoretically $\pi/4$ times the wingspan for an elliptically-loaded wing), and V_0 is the theoretical initial wake descent rate, given as $V_0 = W/2\pi\rho V_{TAS} b^2$, where W refers to aircraft weight, V_{TAS} is the true airspeed, and ρ is the air density. The aircraft weights were assumed to be the maximum takeoff weights of the planes, and the true airspeeds were a conservative estimate of the departure airspeeds in the first few hundred meters AGL, using actual aircraft track data from DFW. A high weight and low airspeed configuration, as is assumed by this analysis, presents the worst case in terms of initial vortex circulation and vortex demise time.

Using the Sarpkaya model, the vortex demise times for several different values of eddy dissipation rate were estimated for several aircraft types, and the results are shown in Figure 10.

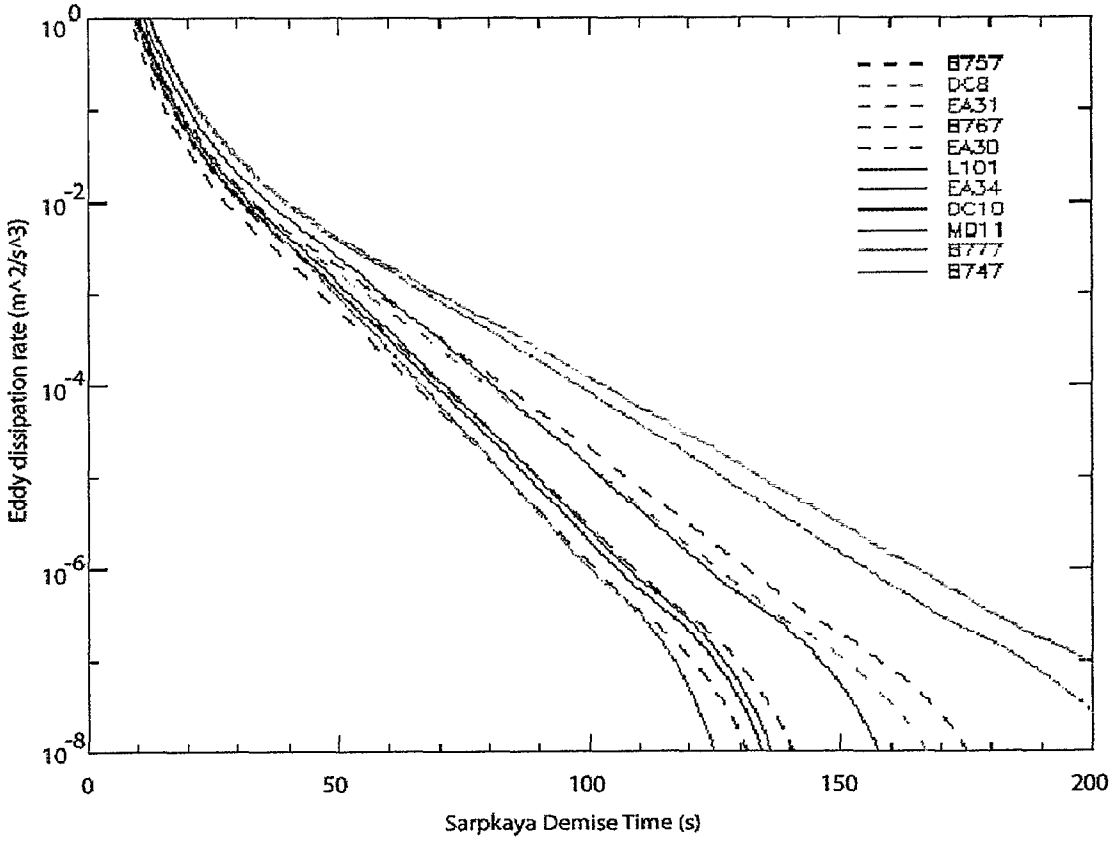

Figure 10. Vortex demise times from the Sarpkaya model as a function of ε for several different aircraft types.

When the vortex demise times from Figure 10 are combined with the probabilities of encountering the dissipation rates, shown in Figure 3, the result is shown in Figure 11. To understand how to interpret the curves in Figure 11, the following example of how these curves are derived is presented. First assume a Sarpkaya demise time of 50 seconds. For most aircraft types, this corresponds to an eddy dissipation rate of ~10^{-3} (from Figure 10). It is known from Figure 3 that away from the ground, the dissipation rate exceeds 10^{-3} about 80% of the time. Therefore, combining these results means that about 80% of the time, the vortex demise times will be ≤ 50 s, as is shown for most aircraft types in Figure 11. When compared to the existing regulation that requires departing aircraft to wait for two minutes following a B757 or Heavy aircraft departure, this result is quite encouraging. It suggests that the weather conditions are conducive to reducing vortex separations on departure most of the time.

Figure 11 also suggests that the selection of a two-minute separation is a judicious choice for a weather-independent spacing requirement. Figure 11 implies that the likelihood of a wake vortex existing beyond two minutes on departure is quite small. The overall odds that a

following aircraft will encounter a wake, if it exists, are even smaller (though NOT zero probability).

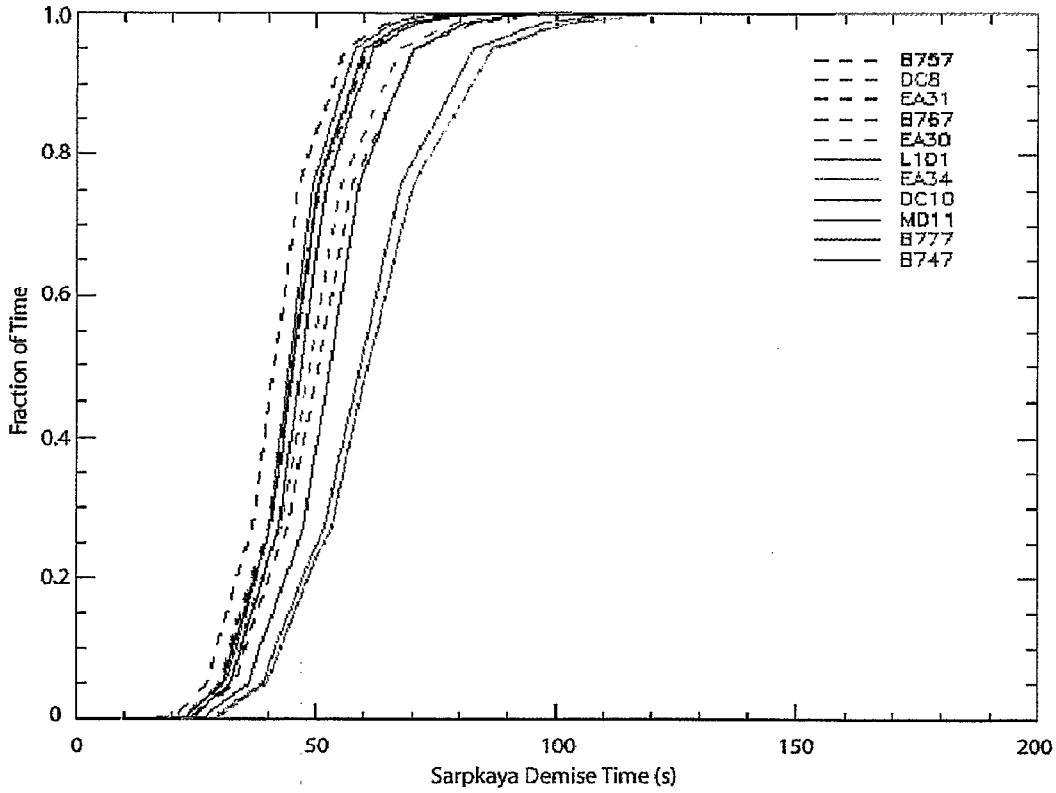

Figure 11. *The fraction of time during the use of a departure wake spacing system that vortex demise would be expected from the Sarpkaya model.*

An important factor in the confidence in the results of Figure 11 is the accuracy of the Sarpkaya model. Though much of the Sarpkaya model is based on measurements, additional studies have been conducted that compare the accuracy of the model with Continuous-Wave LIDAR measurements of aircraft arrivals at MEM and DFW (Joseph, et al., 1999, Robins and Delisi, 1999, Sarpkaya, et al., 2000). As Figure 12 shows, the measurements are consistent with the model trends, although there is considerable scatter in this comparison and there are other formulations that could be considered with similar fits. In this case, the demise time is defined as the time it takes a vortex circulation value to go to 1/e of its initial value as measured by a linear approximation of an exponential to the circulation versus time data.

It is clear from Figure 12 that the model is sufficiently accurate, and the results in Figure 11 are sufficiently dramatic, that it is likely that there is a significant portion of the time that wake vortex separations on takeoff behind B757 or Heavy aircraft can be reduced. These results

will need to be verified by takeoff wake vortex measurements, but takeoff measurements are currently in short supply.

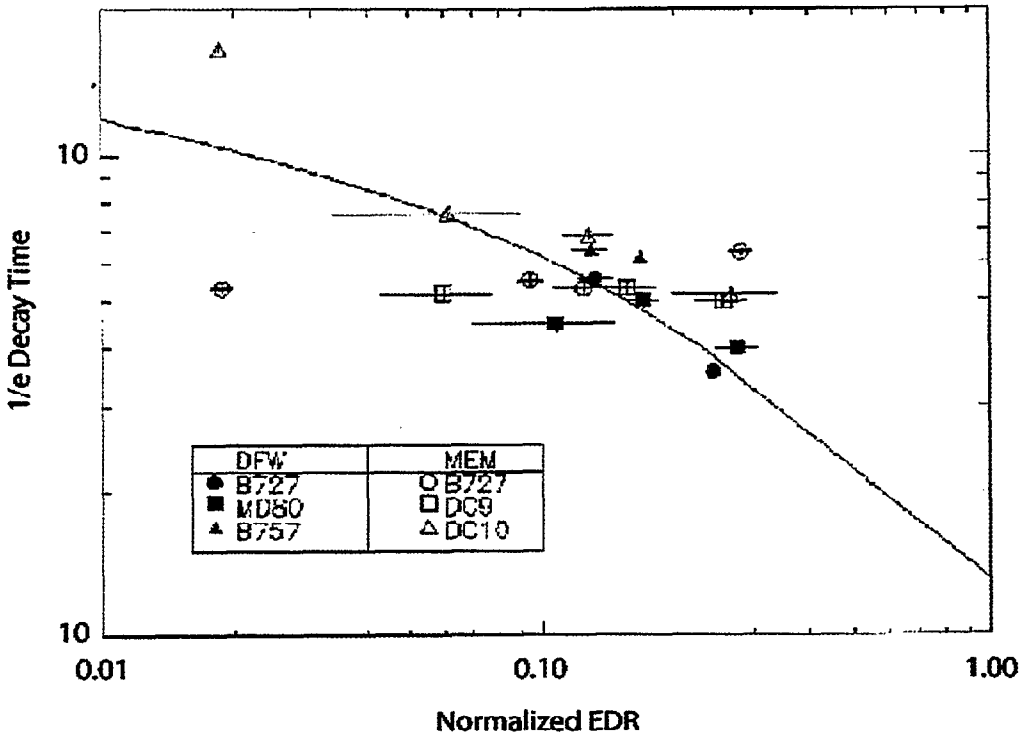

Figure 12. *A comparison of measured wake decay from a Continuous-Wave LIDAR with the predicted decay from the Sarpkaya model (from Joseph, et al., 1999).*

APPENDIX A

The following software written in IDL version 5.2 can be used to compute eddy dissipation rate on the wind data.

```
;-------------------------------------------------------------------------
; Reduce points in PSD by applying an averaging window that increases
; exponentially with frequency. Inputs are the power spectrum psd,
; frequencies f, and time period T. Outputs are the averaged power
; spectrum avg_psd anf the averaged frequencies avg_f.
;-------------------------------------------------------------------------
pro reduce_psd_points,psd,T,f,avg_f,avg_psd
 N=n_elements(psd)
 avg_f = fltarr(5000)
 avg_psd = fltarr(5000)
 del = 0.05
 f_int = 1. / T              ; temporal interval of frequency bins
 log_f_int = alog10(f_int) - del / 2.
 i = 0
 j = fix(alog10(N / 2) / del)
 for k = 0,j do begin
  lowlim = 10^(log_f_int + del * k)
  uplim = 10^(log_f_int + del * (k+1))
  index = where((f ge lowlim) and (f lt uplim),count)  ; total the number of freq pts within window
  if (count ne 0) then begin
   avg_f(i) = total(f(index)) / count
   avg_psd(i) = total(psd(index)) / count
   i = i + 1
  endif
 endfor
 avg_f = avg_f(0:i-1)              ; averaged freq. (Hz)
 avg_psd = avg_psd(0:i-1)          ; averaged psd for u,v,and w comp.
end

;-------------------------------------------------------------------------
; Determine the inertial subrange for each component of the wind
; via separate calls to this function. Lower and upper limit indices (lowlim
; and uplim) and slope of inertial subrange are calculated. Inputs are
; wavenumber k, the power spectrum psd, and the average wind speed windav. The
; slope of the power spectrum over the inertial subrange is returned.
;-------------------------------------------------------------------------
function determine_inertial_subrange,k,psd,windav,lowlim,uplim
;
 slope_tolerance = 0.45
;
; Initial guess at the inertial subrange is a constant range of frequencies, but
; the actual wavenumber range is dependant on the average wind speed.
 k_uplim = 0.5*10.0*2*!pi/windav          ; initial upper limit is Nyquist Frequency
 k_lowlim = 0.3/windav                    ; lower limit is a guess from looking at curves
;
 x = alog10(k)
 y = alog10(psd)
 yy = smooth(y,5)
 slope = (yy-shift(yy,-1))/(x-shift(x,-1))
```

```
 slope = slope(0:n_elements(slope)-2)
 uplim = (where(abs(k-k_uplim) eq min(abs(k-k_uplim))))(0)
 if (uplim gt n_elements(slope)-1) then uplim=n_elements(slope)-1
 lowlim = (where(abs(k-k_lowlim) eq min(abs(k-k_lowlim))))(0)
;
 a=where(slope(lowlim:uplim) lt -1.67+slope_tolerance and slope(lowlim:uplim) $
                gt -1.67-slope_tolerance,act)
 if (act gt 0) then begin
  a=[a,a(n_elements(a)-1)+1]
  uplim=lowlim+a(n_elements(a)-1)
  lowlim=lowlim+a(0)
  xx = x(lowlim:uplim)
  fitslope = regress(reform(xx,1,n_elements(xx)),yy(lowlim:uplim), $
        replicate(1.0,n_elements(xx)),yyfit,/relative_weight)
 endif else begin
  fitslope=9999.0
 endelse

 return,fitslope
end

;-------------------------------------------------------------------------
; Take in a set of U,V,W wind observations and return a new set of
; wind components UU,VV,WW which has been rotated so that UU points in the
; direction of the mean wind, VV points in the primarily horizontal
; cross-component direction, and WW points in the primarily vertical
; cross-component direction.  The average total wind speed (windav)
; is also returned.
;-------------------------------------------------------------------------
pro align_u_with_mean_wind,u,v,w,uu,vv,ww,windav
 uav = total(u)/n_elements(u)
 vav = total(v)/n_elements(v)
 wav = total(w)/n_elements(w)
 windav = sqrt(uav^2 + vav^2 + wav^2)

; Take the mean horizontal wind direction and create u to be in the direction
; of the mean wind and v to be in the direction perpendicular to the mean wind.
 uunit = [uav,vav,wav]/windav
 uu = transpose(uunit)#[reform(u,1,n_elements(u)),reform(v,1,n_elements(v)),$
        reform(w,1,n_elements(w))]
 vunit = [uunit(1),-uunit(0),0.0]
 vv = transpose(vunit)#[reform(u,1,n_elements(u)),reform(v,1,n_elements(v)),$
        reform(w,1,n_elements(w))]
 wunit = crossp(uunit,vunit)
 ww = transpose(wunit)#[reform(u,1,n_elements(u)),reform(v,1,n_elements(v)),$
        reform(w,1,n_elements(w))]
end

;-------------------------------------------------------------------------
; Compute eddy dissipation rate from a 10 Hz sonic anemometer given the
; U, V, and W wind components.  If the dissipation rate cannot be computed
; then the routine returns 9999.0.  Slope is a returned value that can be used to
; see how well the inertial range of the spectrum conforms to the predicted
; -5/3 Kolmogorov slope.
;-------------------------------------------------------------------------
function compute_edr,u,v,w,slope
```

```
  sample_rate = 10.0                              ; number of samples per second (Hz)
  cu = 0.52                                       ; Kolmogorov constant for U' component
  T = float(n_elements(u))/sample_rate   ; total sample time interval (sec)
  f = findgen(n_elements(u)/2 + 1)/T              ; frequency (Hz)
;
  align_u_with_mean_wind,u,v,w,uu,vv,ww,windav
  psd = T*windav*abs(fft(uu-windav,-1))^2/(2*!pi) ; psd of wind comp. (m^3/s^2/rad)
  psd = psd(0:n_elements(u)/2)
  reduce_psd_points,psd,sampint,f,f0,psd0
;
  k0 = 2*!pi*f0 / windav                          ; wavenumber (rad/m)
  slope = determine_inertial_subrange(k0,psd0,windav,lowlim,uplim)
  slope=slope(0)
;
  if (slope ne 9999.0) then begin
    ee = (psd0(lowlim:uplim)*(k0(lowlim:uplim)^(5.0/3))/cu)^1.5
    e=total(ee)/n_elements(ee)
  endif else begin
    e=9999.0
  endelse
;
  return,e
end
```

GLOSSARY

ATC	Air Traffic Control
AVOSS	Aircraft Vortex Spacing System
DFW	Dallas/Ft. Worth Airport
EDR	Eddy Dissipation Rate (ε)
FAA	Federal Aviation Administration
FMS	Flight Management System
IMC	Instrument Meteorological Conditions
LIDAR	Light Detection and Ranging
METAR	Aviation Routine Weather Report (from French)
NASA	National Aviation and Space Administration
MEM	Memphis Airport
TKE	Turbulent Kinetic Energy
VMC	Visual Meteorological Conditions

REFERENCES

Crow, S. C., 1970: "Stability Theory for a Pair of Trailing Vortices", AIAA Journal 8(12): 2172-2179.

Dasey, T. J., 1998: "A Departure Wake Monitoring System: Concept and Benefits", The 2nd U.S.A./Europe Air Traffic Management R&D Seminar ATM-98, http://atm-seminar-98.eurocontrol.fr/.

Dasey, T. J., Campbell, S. D., Heinrichs, R. M., Matthews, M. P., Freehart, R. E., Perras, G. H., and P. Salamitou, 1997: "A Comprehensive System for Measuring Wake Vortex Behavior and Related Atmospheric Conditions at Memphis, Tennessee", Air Traffic Control Quarterly 5(1): 49-68.

Dasey, T. J., Cole, R. E., Heinrichs, R. M., Matthews, M. P., Perras, G. H., 1998: "Aircraft Vortex Spacing System (AVOSS) Initial 1997 System Deployment at Dallas/Ft. Worth (DFW) Airport", Lincoln Laboratory Project Report NASA/L-3, July 8 (available through the National Technical Information Service, Springfield, VA 22161).

Hallock, J. N., Greene, G. C., and Burnham, D. C., 1998: "Wake Vortex Research – A Retrospective Look", Air Traffic Control Quarterly 6(3): 161-178.

Hinton, D. A., Charnock, J. K., and D. R. Bagwell, 2000: "Design of an Aircraft Vortex Spacing System (AVOSS) for Airport Capacity Improvement", AIAA 2000-0622, 38th AIAA Aerospace Sciences Meeting & Exhibit, Jan. 10-13, Reno, NV.

Hogstrom, U., 1996: "Review of Some Basic Characteristics of the Atmospheric Surface Layer", Boundary-Layer Meteorology 78: 215-246.

Joseph, R. M., Dasey, T. J., and R. M. Heinrichs, 1999: "Vortex and Meteorological Measurements at Dallas/Ft. Worth Airport", AIAA 99-0760, 37th AIAA Aerospace Sciences Meeting & Exhibit, Jan. 11-14, Reno, NV.

Lambourne, N. C. and Bryer, D. W., 1961: "The Bursting of Leading-Edge Vortices - Some Observations and Discussions of the Phenomena", ARC-227775, Nat. Phys. Lab., Great Britain. (Also, ARC R&M-3282.)

Perry, R. B., Hinton, D. A., and R. A. Steuver, 1997: "NASA Wake Vortex Research for Aircraft Spacing", AIAA 97-0057, 35th AIAA Aerospace Sciences Meeting & Exhibit, Jan. 9-10, Reno, NV.

Robins, R. E. and Delisi, D. P., 1999: "Further Development of a Wake Vortex Predictor Algorithm and Comparisons to Data", AIAA 99-0757, 37th AIAA Aerospace Sciences Meeting & Exhibit, Jan. 11-14, Reno, NV.

Sarpkaya, T., 1999: "A New Model for Vortex Decay in the Atmosphere", AIAA 99-0761, 37th AIAA Aerospace Sciences Meeting & Exhibit, Jan. 11-14, Reno, NV.

Sarpkaya, T., Robins, R., and Delisi, D., 2000: "Atmospheric Environment Wake-Vortex Eddy Dissipation Model Predictions Compared with Observations", AIAA 2000-0625, 38th AIAA Aerospace Sciences Meeting & Exhibit, Jan. 10-13, Reno, NV.

Vinnichenko, N. K., Pinus, N. Z., Shmeter, S. M., and Shur, G. N 1980: "Turbulence in the Free Atmosphere", translated from Russian by F. L. Sinclair, Consultants Bureau, New York, pp. 15-20.